PHYSICAL REVIEW B VOLUME 25, NUMBER 12 15 JUNE 1982

Calculation of properties of the electron-hole liquid in uniaxially stressed Ge and Si

S. M. Kelso*

Physics Department, University of California, Berkeley, California 94720, Materials and Molecular Research Division, Lawrence Berkeley Laboratory, Berkeley, California 94720, and Bell Laboratories, Murray Hill, New Jersey 07974

(Received 7 December 1981; revised manuscript received 1 March 1982)

We present a detailed theoretical study of the stress dependence of properties of the electron-hole liquid, both at zero and finite temperatures, in $\langle 111 \rangle$-stressed Ge and $\langle 100 \rangle$-stressed Si. These properties include the ground-state equilibrium density, pair energy, electron and hole Fermi energies, sign of the electron-hole drop charge, luminescence linewidth, and liquid compressibility. The results are compared at $T=0$ to the calculations of Kirczenow and Singwi and at $T \approx 2$ K to the available data. We discuss the possibility of a phase transition associated with the depopulation of the upper electron valleys in Ge. We also discuss methods of extrapolating from finite to infinite stress. The importance of the nonparabolicity of the valence bands is emphasized throughout. We discuss ranges of validity for a low-temperature expansion of the free energy. Results are presented for the systematic low-temperature variation of the liquid density, Fermi energy, and chemical potential and for the critical temperature and density. These theoretical results are found to be in reasonably good agreement with available data. Finally, we discuss scaling relations for combinations of electron-hole—liquid properties.

I. INTRODUCTION

The first theories of the electron-hole liquid[1] (EHL) in semiconductors were concerned with predicting and understanding the properties of the EHL for systems in which it had already been observed experimentally, i.e., unstressed Ge and Si.[2–4] It is well known that the band structures of Ge and Si simplify under infinite uniaxial compression: for $\langle 111 \rangle$-stressed Ge only a single conduction-band minimum remains occupied, while for $\langle 100 \rangle$-stressed Si two conduction-band minima remain occupied; in both cases the single populated valence band becomes ellipsoidal. Because of these simplifications, the infinite-stress limit was also considered theoretically.[2,3] These calculations predicted that the EHL would be unbound or just barely bound with respect to free excitons in Ge. However, the more sophisticated calculations of Vashishta *et al.*[5] indicated that the EHL should be observable in the infinite-stress limit. All the calculations predicted that the electron-hole pair density would be considerably reduced compared to that of unstressed crystals. Vashishta *et al.*[6] also performed a calculation for an ideal intermediate-stress case in which the electrons were treated as for infinite stress and the holes as for zero stress; the results were intermediate between the zero- and infinite-stress theories. In addition, the effects of finite temperature on EHL properties and the critical point were estimated for zero and infinite stress, using an expansion valid at low T.[7–9]

In the meantime, several experiments[10–12] were performed to study the EHL in Ge and Si stressed along the three principal crystallographic directions. In these early experiments a stable liquid phase was observed under moderate stresses. Although the luminescence spectra shifted with stress, they were not analyzed in enough detail to determine the properties of the EHL. Experiments performed on inhomogeneously stressed Ge showed that at moderate stresses the electron-hole pair density is reduced from its value in unstressed Ge.[13,14] More recently, systematic experiments have been performed on Ge under $\langle 111 \rangle$ uniaxial stress[15–19] and on Si under $\langle 100 \rangle$ stress[20] to study the stress dependence of EHL properties.

Since experiments cannot be performed at infinite stress or zero temperature, it is clearly desirable to have a finite-stress, finite-temperature theory. A first attempt to predict the systematic variation of the ground state ($T=0$ K) properties of the EHL in $\langle 111 \rangle$-stressed Ge was made by Mar-

 ©1982 The American Physical Society

kiewicz and Kelso.[21] In that paper, the stress dependence of the holes was taken into account but the electrons were treated as for infinite stress, so the results are valid only for the intermediate- to high-stress range. Liu *et al.*[22,23] performed a calculation for two values of the stress, for both Ge and Si, and included a low-T expansion to estimate the critical point. Kirczenow and Singwi have considered the systematic stress dependence of some EHL properties in Ge (Ref. 24) and Si (Ref. 25), restricted to $T=0$.

In this paper we present detailed calculations[26,27] of the properties of the electron-hole liquid as a function of compressive $\langle 111 \rangle$ stress in Ge and $\langle 100 \rangle$ stress in Si, both at $T=0$ and finite temperature. We include the full stress dependence of the conduction and valence bands in the kinetic energy, except that the split-off valence band is ignored. Energy- and stress-dependent hole masses, introduced previously,[14,21,28] are used to describe the nonparabolicity of the valence bands. We initially consider several models for the exchange-correlation energy; two include separate stress and density dependences. We compare the exchange-correlation energies directly, as well as results for the EHL ground-state density and energy. Two models are selected for further calculations and for comparison with experiment. We believe that uncertainty in the mathematical representation of the correlation energies of Vashishta *et al.* can result in model-dependent predictions. Consequently, one of the models selected for our detailed calculations uses a simple empirical correlation energy. Both models are different from those considered by Kirczenow and Singwi.[24,25]

Results are presented for several properties of the EHL at $T=2$ K to facilitate comparison with experiment. In addition to the density, we discuss the electron and hole Fermi energies, the sign of the charge on electron-hole drops (EHD), and the binding energy ϕ of the EHL with respect to free excitons. While there is overall qualitative agreement between theory and experiment, some quantitative differences are discussed.

It is convenient to introduce two critical values of stress. When the stress-induced splitting of the conduction bands E^e_{spl} is equal to the electron Fermi energy E^e_F, the upper electron valleys are depopulated (at $T=0$). Thus a critical stress σ_e is determined by the condition $E^e_{\mathrm{spl}}=E^e_F$. Similarly, a critical stress σ_h, associated with the emptying of one valence band, is defined by the condition $E^h_{\mathrm{spl}}=E^h_F$.

In agreement with Kirczenow and Singwi,[24,25] we find a rapid decrease in the electron-hole pair density associated with the emptying of the upper conduction bands at σ_e. For Ge at $T=0$, we discuss the possibility of two different types of EHL, with a phase transition as a function of stress. Our model-dependent results indicate a critical dependence on details of the exchange-correlation energy, such as curvature with respect to density, which are not well known. We show by explicit calculation that the change in the number of occupied conduction bands is an important factor in the possibility of a discontinuous change in the equilibrium density at σ_e; thus the unambiguously more gradual density change predicted for Si is understood.

We predict significant changes in all EHL properties for stresses beyond σ_h. Since no further changes take place in the number of occupied bands, the high-stress variation of EHL properties arises solely from the residual nonparabolicity of the valence band, which remains important even after the bands are well split in energy. Because these variations continue well past σ_h, we discuss procedures for extrapolating finite-stress data to the infinite-stress limit.

For finite temperatures, both low-T and high-T limits are considered. At sufficiently low temperatures we find that the usual expansion for the kinetic energy of a degenerate Fermi system is valid, except at stresses very near σ_e and σ_h. We discuss the systematic low-T variation of EHL properties, using derivatives of the ground-state free energy versus density. Near the critical point, however, we find that the expansion is no longer valid at any stress. Thus we calculate the kinetic energy exactly at all finite temperatures. Our theoretical results are compared with available data. In addition, we consider scaling relations of certain combinations of EHL properties as the band structure changes with stress.

The paper is divided into several sections. The calculation of the free energy of electrons and holes at arbitrary stress and temperature is described in Sec. II. Results for ground-state EHL properties are presented in Sec. III. Finally, results for finite temperatures are presented in Sec. IV.

II. FORMALISM: THE FREE ENERGY AT ARBITRARY STRESS AND TEMPERATURE

The free energy F of a neutral plasma of electrons and holes is a function of the number of

electron-hole pairs N, volume V, and the lattice temperature T. The free energy has kinetic and exchange-correlation energy contributions, which are treated separately.

A. Kinetic energy

The kinetic energy term is just the free energy for a gas of free Fermi particles. For carriers in a band with a density of states $D(E)$,

$$F=NE_F-PV$$
$$=NE_F-\int_0^\infty\left[\int_0^E D(u)du\right](1+e^{(E-E_F)/kT})^{-1}dE\ , \tag{1}$$

where the second term is the grand potential, $\Omega\equiv -PV$, and P is the pressure. The Fermi energy E_F is determined by the relation

$$N=\int_0^\infty D(E)(1+e^{(E-E_F)/kT})^{-1}dE \tag{2}$$

and depends on temperature. The density of states contains information about the band structure. It is convenient to write[28]

$$D(E)=\frac{\sqrt{2}V}{\pi^2\hbar^3}m_{\mathrm{dloc}}^{3/2}(E)\,E^{1/2}\ , \tag{3a}$$

where $m_{\mathrm{dloc}}(E)$ is a local density-of-states mass:

$$m_{\mathrm{dloc}}^{3/2}(E)\equiv\frac{\hbar^3}{4\sqrt{2}\pi E^{1/2}}\int k^2\frac{dk}{dE}d\Omega\ . \tag{3b}$$

The integration is performed over solid angle on the k-space surface with energy E. m_{dloc} depends on energy if the band is nonparabolic, as is the case for the valence bands in Ge or Si at finite stress. Results for $\langle 111\rangle$-stressed Ge and $\langle 100\rangle$-stressed Si are given in Figs. 1(c) and 2(a) of Ref. 28. These results were fit to simple analytic functions over several ranges of reduced energy $E'\equiv E/\sigma$, matching the functions and their first derivatives between ranges. The conduction band is assumed to be parabolic, with the same density-of-states mass at all stresses.

In Ge and Si the conduction and valence bands are split by the stress, with only the band(s) lowest in energy remaining populated at high stress. For a set of $\nu_1+\nu_2$ bands, with ν_1 bands split by an energy E_{spl} below the other ν_2 bands, Eq. (3a) becomes

$$D(E)=\frac{\sqrt{2}V}{\pi^2\hbar^3}[\nu_1 m_1^{3/2}(E)E^{1/2}+\nu_2 m_2^{3/2}(E)(E-E_{\mathrm{spl}})^{1/2}]\ , \tag{4}$$

where $m_1(E)$ and $m_2(E)$ are the local density-of-states masses and E is measured from the bottom of the band for set 1. It is understood that $m_2(E)=0$ for $E<E_{\mathrm{spl}}$. We use the same Fermi level for both subsets, indicating that all the carriers are in thermal equilibrium with each other. This corresponds to the equilibrium limit of Kirczenow and Singwi.[24]

The procedure for calculating the kinetic energy was as follows: (1) a hole Fermi energy E_F^h was chosen; (2) the density $n\equiv N/V$ was computed using Eq. (2) for holes; (3) the electron Fermi energy E_F^e was obtained by inverting Eq. (2) for electrons; (4) $F_{\mathrm{kin}}=F_{\mathrm{kin}}^e+F_{\mathrm{kin}}^h$ was computed using Eq. (1). We usually wanted to find a minimum in the total pair free energy $f(n)\equiv F/N$ or the disappearance of a minimum in the chemical potential $f(n)\equiv f+n\partial f/\partial n$. These minima were often very shallow: To determine the equilibrium density at $T=0$ to within 1% it was necessary to calculate $f(n)$ to a precision of 1 part in 10^6. Of course, the band-structure parameters are not known this well, but it was desirable to reduce the mathematical uncertainties.

At finite temperature the kinetic energy was computed exactly, rather than using the T^2 expansion employed by other authors[7,8,23] (see discussion in Sec. IV B). We note that the integrals in Eqs. (1) and (2) become (modified) Fermi-Dirac integrals for the electrons (holes) and must be evaluated numerically.

B. Exchange-correlation energy

A detailed first-principles calculation of the exchange-correlation energy, including the effects of finite stress and temperature, would be mathematically formidable and has not been attempted. First, as in many other calculations,[7–9,23,29–32] we suppose that the exchange-correlation energy is independent of T and use results for $T=0$. This is reasonable as long as kT is much less than the plasmon energy $\hbar\omega_p$,[9,33] where $\omega_p^2=4\pi ne^2/m^*$. For such an excitation m^* is an optically averaged mass given by[34] $m_0/m^*=m_0/m_{\mathrm{oe}}+m_0/m_{\mathrm{oh}}$. We shall see in Sec. IV B that this condition is fulfilled for all temperatures of interest here. In addition, it has been observed[35,36] that the exchange-correlation energy is nearly independent of such band-structure features as mass, anisotropy, and degeneracy, as long as both the exchange and correlation energies are calculated using the *same* details. The separate dependences of the exchange and correla-

tion energies on the band structure can be substantial but tend to cancel in the sum.[37] This cancellation has been exploited in some $T=0$ calculations.[21,24,25,35] In addition, Vashishta has suggested[38] that the correlation energy should depend only weakly on the hole mass. We investigate both the cancellation and the hole mass dependence here.

We initially considered six models for the exchange-correlation energy, summarized in Table I. In several models the electrons and holes are independently treated as for zero or infinite stress. In this case the exchange energy per electron-hole pair is given by

$$f_{\rm ex}=-\frac{3e^2}{4\pi\kappa}(3\pi^2 n)^{1/3}\left[\frac{\phi(\rho_e)}{\nu_e^{1/3}}+\psi(\rho_h)\right], \quad (5)$$

where ν_e is the number of electron valleys and $\rho=m_t/m_l$ is the electron or hole anisotropy parameter. Values for $\phi(\rho_e)$ and $\psi(\rho_h)$ are listed in Table II, along with other parameters used in the calculations.

The scheme used for models 1 and 2 (Ref. 21) (infinite-stress electrons, zero-stress holes) most closely represents an intermediate stress[6,39] near σ_e, although it does not correspond exactly to any value of stress. The model 1 correlation energy uses the results of a detailed numerical calculation[38,40] in a fully self-consistent (FSC) approximation[4,5,7] including multiple scattering and band anisotropy. The results were fit to a polynomial in the interparticle spacing r_s for higher densities and matched to a Wigner form for lower densities.[40] In model 2, this detailed calculation is replaced by a simple empirical correlation energy, taken to be a sum of Wigner-type contributions from the electrons and holes[41]:

$$f_{\rm corr}=-\frac{c}{n^{-1/3}+a/m_{\rm oe}}-\frac{c}{n^{-1/3}+a/m_h}, \quad (6)$$

where $m_{\rm oe}$ is the electron optical mass and m_h is a hole mass, here the infinite-stress optical mass. The constants a and c are chosen to match the value and first derivative of Eq. (6) to the model 1 correlation energy at the equilibrium density for infinite-stress electrons and zero-stress holes in the kinetic energy. Values for a,c, and the masses are given in Table II.

In models 3 (Ref. 21) and 4 the hole mass in Eq. (6) varies with both density and stress.[27] In model 3 m_h is the optical mass while in model 4 it is the integrated density-of-states mass, in both cases averaged over two hole bands.[28] Models 5 and 6 are FSC results[39] for extreme cases (zero and infinite stress, respectively) in which both the exchange and correlation energies are calculated using the same band-structure details. These models are similar to those considered by Kirczenow and Singwi.[24,25,35]

Variations among the exchange-correlation energies may be investigated by considering ratios of different models. Models 1, 2, 5, and 6, in which the density dependence is independent of stress, are compared in Fig. 1 for Si. Model 2 was selected as the normalization model because it uses a simpler form for the correlation energy. The FSC models exhibit small oscillations (artifacts of the fitting polynomials) relative to model 2. While these oscillations do not occur in the individual exchange-correlation energies, it is nevertheless clear that the *curvature* may not be well represented in the FSC models. This will be important for the calculation

TABLE I. Electron and hole treatments in the exchange-correlation energy models.

Model	Type	Exchange energy Electrons	Exchange energy Holes	Correlation energy Electrons	Correlation energy Holes
1	FSC	infinite stress	zero stress	infinite stress	zero stress
2	Wigner	infinite stress	zero stress	infinite stress	infinite-stress optical mass
3	Wigner	infinite stress	zero stress	infinite stress	stress-dependent optical mass
4	Wigner	infinite stress	zero stress	infinite stress	stress-dependent density-of-states mass
5	FSC	zero stress	zero stress	zero stress	zero stress
6	FSC	infinite stress	infinite stress	infinite stress	infinite stress

TABLE II. Parameters used in the calculations.

Parameter	Ge	Ref.	Si	Ref.
Electrons				
$m_{\rm et}/m_0$	0.08152	a	0.1905	b
$m_{\rm el}/m_0$	1.588	a	0.9163	b
$m_{\rm de}/m_0$	0.2193	c	0.3216	c
$m_{\rm oe}/m_0$	0.1192	d	0.2588	d
$\phi(\rho_e)$	0.8401	e	0.9490	e
ν_e (zero stress)	4		6	
ν_e (infinite stress)	1 (⟨111⟩ stress)		2 (⟨100⟩ stress)	
$-E^e_{\rm spl}/\sigma$	1.05	f	0.86	f
Holes				
$\psi(\rho_h)$ (zero stress)	0.710	g	0.746	g
$-E^h_{\rm spl}/\sigma$	0.362	h	0.272	h
Holes: infinite stress	⟨111⟩ stress		⟨100⟩ stress	
$m_{\rm ht}/m_0$	0.1302	i	0.2561	i
$m_{\rm hl}/m_0$	0.040 37	i	0.1989	i
$m_{\rm dh}/m_0$	0.088 11	c	0.2354	c
$m_{\rm oh}/m_0$	0.074 74	d	0.2337	d
$\psi(\rho_h)$	0.9698	e	0.9986	e
Miscellaneous				
κ	15.36	j	11.40	j
a (model 2)	0.1917	k	0.2128	k
c (model 2)	4.461	k	8.552	k

[a]B. W. Levinger and D. R. Frankl, J. Phys. Chem. Solids 20, 281 (1961).
[b]J. C. Hensel, H. Hasegawa, and M. Nakayama, Phys. Rev. 138, A225 (1965).
[c]$m_d=(m_t^2 m_l)^{1/3}$ for electrons or holes.
[d]$m_o^{-1}=\frac{1}{3}(2m_t^{-1}+m_l^{-1})$ for electrons or holes.
[e]M. Combescot and P. Nozières, J. Phys. C 5, 2369 (1972).
[f]Units: meV mm^2/kgf. For ⟨111⟩ stress (Ge), $-E^e_{\rm spl}/\sigma=4\Xi_u/9C_{44}$. For ⟨100⟩ stress (Si), $-E^e_{\rm spl}/\sigma=\Xi_u/(C_{11}-C_{12})$. Values for Ξ_u are from I. Balslev, Phys. Rev. 143, 636 (1966). Values for the C's for Ge are from M. E. Fine, J. Appl. Phys. 26, 862 (1965) ($T=1.7$ K). Values for the C's for Si are from H. J. McSkimin, J. Appl. Phys. 24, 988 (1953) ($T=78$ K values multiplied by 1.002 to extrapolate to low temperature).
[g]W. F. Brinkman and T. M. Rice, Phys. Rev. B 7, 1508 (1973).
[h]Units: meV mm^2/kgf. For ⟨111⟩ stress (Ge), $-E^h_{\rm spl}/\sigma=d/\sqrt{3}C_{44}$. For ⟨100⟩ stress (Si), $-E^h_{\rm spl}/\sigma=2b/(C_{11}-C_{12})$. Values for d (Ge) and b (Si) are from J. C. Hensel and K. Suzuki, Phys. Rev. B 9, 4219 (1974) and from J. C. Hensel and G. Feher, Phys. Rev. 129, 1041 (1963), respectively. Values for the C's are as in Ref. f.
[i]Calculated from Ge and Si valence-band structures: see S. M. Kelso, Phys. Rev. B 25, 1116 (1982).
[j]R. A. Faulkner, Phys. Rev. 184, 713 (1969).
[k]Model 2 is described in the text. If n has units 10^{17} cm^{-3} and the masses are multiples of the free-electron mass, then a is dimensionless and c is in meV.

of the critical point and is discussed further, along with the dashed curve, in Sec. IV B.

III. RESULTS: GROUND-STATE PROPERTIES

In this section we present results for the ground-state properties of the electron-hole liquid in ⟨111⟩-stressed Ge and ⟨100⟩-stressed Si. We compare results for the six models with each other and with other calculations, discuss a possible phase transition associated with the emptying of the upper electron valleys in Ge, compare the results at $T=2$ K with the available data, and give

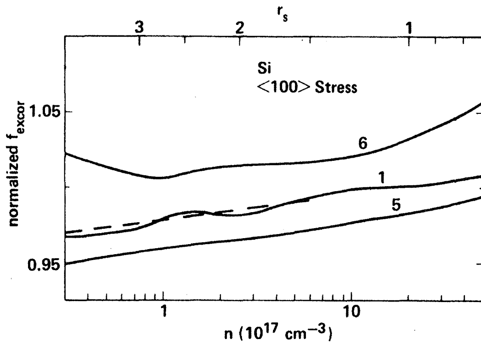

FIG. 1. Exchange-correlation energy per electron-hole pair for models 1, 5, and 6, normalized to model 2, for ⟨100⟩-stressed Si. The dashed curve is discussed in Sec. IV B.

guidelines for extrapolating to the infinite-stress limit.

A. Comparison of models

The ground state of the EHL occurs at the density for which the free energy per electron-hole pair is a minimum at $T=0$ K. The ground-state densities n_0 are shown as a function of compressive stress σ for Ge in Fig. 2. As is conventional, compressive stresses are negative and are expressed in kgf/mm^2, where 1 kgf=9.806 65 newtons. Part (a) shows the results for FSC-based models while part (b) shows the results for Wigner-type models. Arrows indicate the values which should be most nearly correct at zero and infinite stress (models 5 and 6, respectively). The results for Si are qualitatively similar (see also Fig. 8).

All the models for both materials show the same general trends with stress: (1) A fairly rapid decrease in density occurs near the critical stress σ_e, where $E_F^e = E_{\rm spl}^e$. The density change is larger for Ge due to the greater change in the number of occupied valleys. (2) The density remains nearly constant between σ_e and σ_h, where $E_F^h = E_{\rm spl}^h$. As shown below, $-\sigma_h \approx 6$ kgf/mm^2 for Ge. (3) A slight kink occurs at σ_h, followed by a further gradual decrease which is still apparent at much higher stresses. We find that n_0 changes by over a factor of 2 in Si and by approximately a factor of 4 in Ge *after* σ_h. In models 1, 2, 5, and 6 this stress dependence comes entirely from the hole kinetic energy, arising from the residual nonparabolicity of the occupied ($|M_J| = \frac{1}{2}$) valence band. Thus the valence bands do not decouple until they are split quite far apart in energy[21,22,27] (see also Sec. III C). The oscillation in model 3 is associated with a local maximum in the hole optical mass used in the correlation energy.[21,27]

Our results may be compared to other calculations. Model 6 is virtually identical to one model used by Kirczenow and Singwi[24,25] and is similar to the model used by Liu *et al.*[22,23]; the results are correspondingly similar. The other models used in Refs. 24 and 25 differ somewhat from the present models. We note that we have used deformation potentials for Si which are different from those implied in Ref. 25. As shown in Table II, the deformation potentials used here yielded a ratio $E_{\rm spl}^e / E_{\rm spl}^h = 3.2$, compared to a ratio of 1.8 used by Kirczenow and Singwi.[42] For Ge we used $E_{\rm spl}^e / E_{\rm spl}^h = 2.9$, in agreement with the value used in Ref. 24.

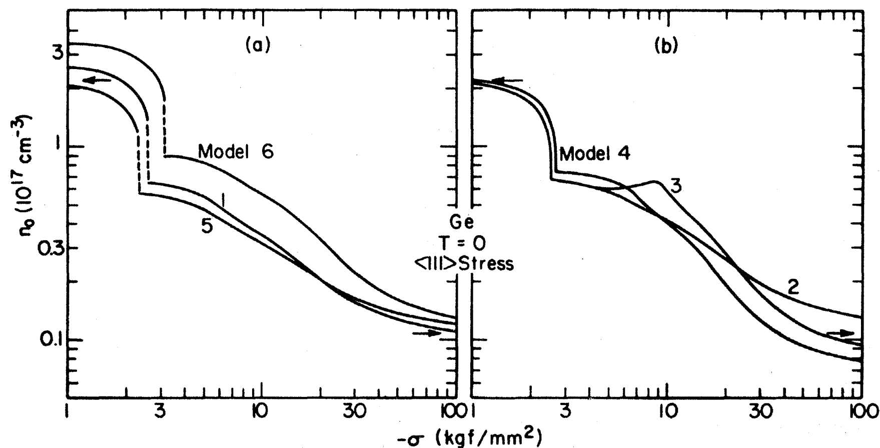

FIG. 2. Ground-state density n_0 vs stress σ for the EHL in ⟨111⟩-stressed Ge. (a) models 1, 5, and 6; (b) models 2, 3, and 4. The arrows indicate the model 5 zero-stress and model 6 infinite-stress densities.

The ground-state energy per pair, f_G, is shown for Ge in Fig. 3; results for Si are again qualitatively similar. A rather sudden change in slope occurs at σ_e. The EHL is bound with respect to free excitons if $|f_G|$ is greater than the exciton binding energy E_x. For infinite stress E_x is the excitonic Rydberg,[43] which is 2.65 meV for Ge and 12.85 meV for Si. A dashed line is shown in the figure. Our calculations predict an unbound liquid state for models 3 and 4 above $-\sigma \approx 23$ and 13 kgf/mm^2, respectively, in Ge and for model 4 above $-\sigma \approx 44$ kgf/mm^2 in Si. At low stresses the exciton structure is complicated due to the valence-band degeneracy and the conduction-band anisotropy.[44] Experimental values for the binding energy of the lowest zero-stress exciton state are 4.15 meV for Ge (Ref. 45) and 14.7 meV for Si (Ref. 46). Independent of the details of the variation of E_x at intermediate stress, which has been neither measured nor calculated, the binding energy ϕ of the liquid with respect to free excitons is expected to decrease rather rapidly with stress at low stresses. This effect has been observed both in Ge (Ref. 47) and in Si (Refs. 20 and 48).

For further calculations we will not consider so many models. We note that a bound liquid state has been observed in both Ge and Si at high stresses where models 3 and/or 4 do not predict binding. In addition, since the hole mass variations in models 3 and 4 were omitted from the exchange energy, these models probably overestimate the effect of the hole mass on the exchange-correlation energy. Among the FSC-based models, we select model 1 as an average. The Wigner-based model 2 provides a useful complement since the correlation energies agree in value and slope at one point but have different curvatures. Thus models 1 and 2 will be compared in detail.

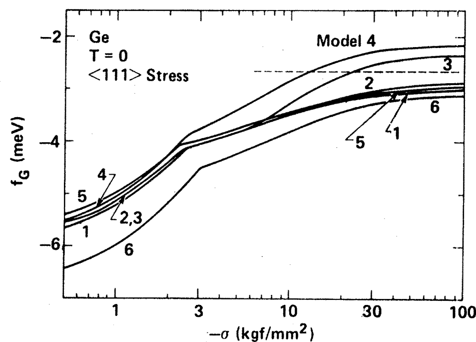

FIG. 3. Ground-state electron-hole pair energy vs stress for the EHL in ⟨111⟩-stressed Ge. The dashed line is the infinite-stress exciton binding energy.

Numerical results for several ground-state properties of the EHL are listed in Table III for selected stress values for models 1 and 2. In addition the model 5 zero-stress and model 6 infinite-stress results are listed, along with experimental values for zero stress.[1] The first stress is slightly greater than $-\sigma_e$, so that the upper electron valleys are depopulated. Similarly, the second stress is slightly greater than $-\sigma_h$, so that only one valence band is populated. The final stress is a few times $-\sigma_h$ and illustrates that further changes occur before the high-stress limit is attained.

B. Possible phase transition in Ge near σ_e

We noted in the preceding section that a rapid change in the equilibrium density occurs just below the critical stress σ_e. Our detailed calculations for models 1, 5, and 6 in Ge showed[27] that the pair free energy has two minima in a very narrow range of stresses ($\Delta\sigma \lesssim 0.1$ kgf/mm^2) around σ_e. At $T=0$, the true ground state of the system is associated with the minimum having the lowest energy f_G. As the stress changes the relative energies of the two minima change. Thus the calculations predict a discontinuous decrease in n_0 (i.e., a phase transition) as the stress increases. This is indicated in Fig. 2(a) by dashed lines. The possibility of such a discontinuous change in density was noted independently by Kirczenow and Singwi[24] but seems less clear for the equilibrium limit in their calculations.

The prediction of a double minimum in the free energy for Ge is not model independent: models 2–4 predict a *rapid but continuous* change in n_0 [see Fig. 2(b)]. Andryushin *et al.*[49] used a model in which the valence-band changes were ignored and which employed a Combescot-Nozières form[2] of the correlation energy; they found no phase separation. On the other hand, Kastal'skii's Hartree-Fock calculation (no correlation energy) does predict a double minimum.[50] Corresponding calculations for ⟨100⟩-stressed Si (Refs. 25, 27, and 49) predict that the double minimum does not occur for that system.

We examined the free energy curves for Ge in some detail[27] and found that the height of the energy barrier between the two minima was very small, less than ~ 0.004 meV or 0.05 K. Whether two minima occur, as in model 1, or only one minimum, as in model 2, depends very sensitively on the details of $f_{\text{corr}}(n)$ in the range $n \approx (0.6-1.5) \times 10^{17}$ cm^{-3}. The ratio of the

TABLE III. Selected numerical results for the ground-state properties of the EHL in stressed Ge and Si.

Material, Stress direction	$-\sigma$ (kgf/mm^2)	Model	n_0 (10^{17} cm^{-3})	$-f_G$ (meV)	E_F^e (meV)	E_F^h (meV)	$K_T(n_0)$ (cm^2/dyne)
Ge, $\langle 111 \rangle$	Zero	Expt.[a]	2.3 ± 0.1	6.1 ± 0.2	2.53 ± 0.02	3.90 ± 0.02	$(2.3\pm0.6)\times10^{-3}$
		5	2.21	5.88	2.40	3.73	3.12×10^{-3}
		1	2.70	6.14	2.75	4.27	2.31×10^{-3}
		2	2.24	6.03	2.43	3.77	2.87×10^{-3}
	3	1	0.642	4.06	2.66	2.16	1.80×10^{-2}
		2	0.659	4.06	2.71	2.19	1.38×10^{-2}
	7	1	0.435	3.66	2.05	2.32	3.75×10^{-2}
		2	0.492	3.65	2.23	2.45	2.42×10^{-2}
	20	1	0.200	3.22	1.22	2.19	9.05×10^{-2}
		2	0.259	3.15	1.45	2.49	5.98×10^{-2}
	Infinite	1	0.098	2.96	0.76	1.92	1.25×10^{-1}
		2	0.112	2.82	0.83	2.10	1.09×10^{-1}
		6	0.109	3.07	0.81	2.06	1.39×10^{-1}
Si, $\langle 100 \rangle$	Zero	Expt.[a]	33 ± 1	23	7.8 ± 0.1	14.4 ± 0.1	$(3.4\pm2)\times10^{-5}$
		5	32.3	21.97	7.50	13.79	5.96×10^{-5}
		1	31.8	22.52	7.43	13.64	6.69×10^{-5}
		2	29.3	22.42	7.03	12.91	6.47×10^{-5}
	12	1	13.6	17.42	8.75	9.32	1.58×10^{-4}
		2	13.1	17.42	8.55	9.14	1.78×10^{-4}
	40	1	9.04	15.47	6.68	10.25	2.88×10^{-4}
		2	8.18	15.54	6.25	9.74	3.98×10^{-4}
	100	1	6.22	14.60	5.20	9.94	4.22×10^{-4}
		2	5.41	14.78	4.74	9.17	5.63×10^{-4}
	Infinite	1	4.74	14.09	4.34	9.46	5.50×10^{-4}
		2	4.20	14.35	4.01	8.73	6.40×10^{-4}
		6	4.46	14.71	4.17	9.08	5.99×10^{-4}

[a]The experimental data at zero stress are compiled from J. C. Hensel, T. G. Phillips, and G. A. Thomas, *Solid State Physics,* edited by H. Ehrenreich, F. Seitz, and D. Turnbull (Academic, New York, 1977), Vol. 32, p. 88.

exchange-correlation energies for models 1 and 2 varies between 1.000 and only 1.005 in this range. It is difficult to distinguish between the mathematical representations on a first-principles basis.

For $\langle 100 \rangle$-stressed Si, the density decrease associated with the depopulation of the upper electron valleys is smaller and more gradual than for Ge. The change in the number of populated conduction bands is smaller in Si. To investigate the effect of the relative change in the number of occupied conduction bands, a series of artificial models was constructed, similar to model 1 for Ge, with the number ν_2 of upper electron valleys a parameter. The ground-state equilibrium densities for several models with ν_2 ranging from 1 to 9 are shown in Fig. 4; $\nu_2=3$ corresponds to Ge, while $\nu_2=2$ corresponds (qualitatively) to Si. It is clear that a large relative change in the conduction-band degeneracy, which is accompanied by a rapid variation in the

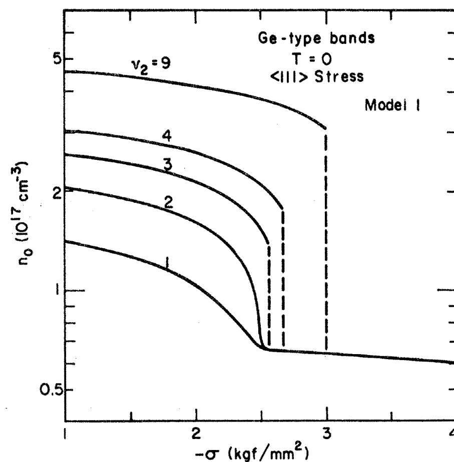

FIG. 4. Equilibrium density vs stress for Ge-like bands with one lower and ν_2 upper electron valleys. The model 1 exchange-correlation energy is used.

electron kinetic energy, tends to favor the formation of a double minimum.

It would be very interesting if nature provided a real system with a large change in a band degeneracy. In the alloy $Ge_{1-x}Si_x$, with $x \approx 0.15-0.20$, the four Ge-like $\langle 111 \rangle$ conduction-band minima and the six Si-like $\langle 100 \rangle$ minima are degenerate.[51] With the application of $\langle 111 \rangle$ uniaxial stress the $\langle 100 \rangle$ valleys would remain degenerate while the $\langle 111 \rangle$ valleys would become stress split. Thus the number of EHL-occupied conduction bands would change from 10 to 7 to 1 for increasing $\langle 111 \rangle$ stress. Other indirect semiconductor alloys in which the $\langle 111 \rangle$- and $\langle 100 \rangle$-associated minima become degenerate include the III-V pseudobinaries $In_{1-x}Ga_xP$ ($x \approx 0.77$) (Ref. 52) and $Al_xGa_{1-x}Sb$ ($x \approx 0.56$) (Ref. 53). Although the EHL has not yet been observed in the latter materials, an experimental study of such a system would provide valuable insight into the nature of this proposed phase transition.

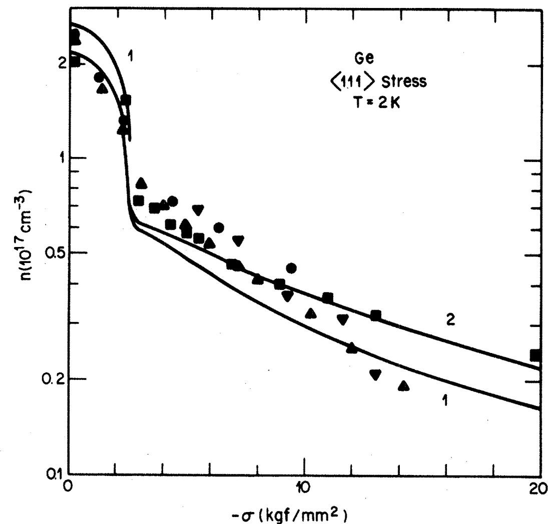

FIG. 5. Equilibrium density vs stress for Ge at $T=2$ K. The curves are the results for models 1 and 2. The data points are taken from Refs. 18 (●), 16 (▼), 17 (▲), 14 (+), and 19 (■).

C. Comparison with experiment: The approach to the infinite-stress limit

Because experiments are typically performed with the sample immersed in pumped liquid helium, the calculations have been redone for $T=2$ K using the procedure described in Sec. II. At $T=2$ K the equilibrium density is still given very accurately by the free-energy minimum.

We consider first the results for $\langle 111 \rangle$-stressed Ge. Figure 5 shows the theoretical equilibrium density along with several sets of data. Note that model 1 predicts a discontinuous density change at σ_e even at $T=2$ K, but we find that the energy barrier between the minima is even lower than at $T=0$. The experimental densities were obtained by fitting luminescence spectra from the EHL in uniaxially stressed Ge (Refs. 16–18) or from the strain-confined EHL (Ref. 14) or by fitting plasma resonance line shapes for uniaxially stressed samples.[19] In all cases the line-shape analyses were performed using the appropriate energy- and stress-dependent hole masses.[27,28] Overall, theory and experiment are in reasonable agreement. The density decrease associated with the emptying of the upper electron valleys is not as pronounced in the data as in the theory. However, a decrease of a factor of 2 in density has been observed within a very narrow stress range, less than half a kgf/mm^2, by Zarate and Timusk.[19]

While the data of Zarate and Timusk agree very nicely with model 2, the data of Feldman *et al.*[16] and of Chou and Wong[17] decrease more rapidly at higher stresses than the predictions of either model. Although care was taken to assure stress uniformity in the experiments, we note that residual nonuniformity will result in broader spectra and higher deduced densities. Thus, if the stress calibrations are accurate and if comparable line-shape analyses are performed, the narrower spectrum and lower density should be more nearly correct.

The EHL work function ϕ has been measured spectroscopically from EHL and exciton luminescence spectra at two stresses. Furneaux *et al.*[14,54] found $\phi \approx 1$ meV at $-\sigma \approx 6$ kgf/mm^2. A theoretical upper limit to ϕ is obtained using the infinite-stress E_x; we find $\phi \lesssim 1.15$ meV for both models. In addition, Feldman *et al.*[15] measured $\phi = 0.65 \pm 0.07$ meV at $-\sigma = 13$ kgf/mm^2, compared to 0.82 meV for model 1 and 0.77 meV for model 2. The agreement is quite satisfactory.

The electron and hole Fermi energies, E_F^e and E_F^h, are shown in Fig. 6. The dashed lines are the conduction- and valence-band splittings, $E_{\rm spl}^e$ and $E_{\rm spl}^h$. The critical stresses, determined by the relations $E_F = E_{\rm spl}$, are

$$\left.\begin{array}{l} -\sigma_e \approx 2.5 \text{ kgf/mm}^2 \\ -\sigma_h \approx 6 \text{ kgf/mm}^2 \end{array}\right\} \text{Ge}, \; T=2 \text{ K}, \; \langle 111 \rangle \text{ stress} \qquad (7)$$

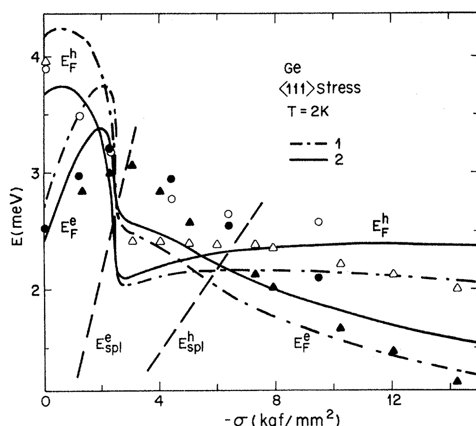

FIG. 6. Electron and hole Fermi energies E_F^e and E_F^h vs stress for Ge at $T=2$ K. The dot-dashed curves are model 1, while the solid curves are model 2. The dashed lines indicate the energy splitting E_{spl} between upper and lower bands for electrons and for holes. The data points for E_F^e (solid symbols) and E_F^h (open symbols) are from Ref. 18 (circles) and Ref. 17 (triangles).

for both models. At low stresses, the electron Fermi energy is forced to increase as the upper electron valleys begin to depopulate; the hole Fermi energy decreases gradually as the density decreases. The changes in the electron kinetic energy become increasingly important near σ_e, and the density and both Fermi energies decrease rapidly. Above σ_e, E_F^e decreases smoothly, tracking the density, since there are no further changes in the conduction-band structure. The changes in the hole Fermi energy between σ_e and σ_h reflect the changes in the population of the $|M_J|=\frac{3}{2}$ valence band and in the hole mass. Above σ_h the decrease in E_F^h and n is due to the decrease in the density-of-states hole mass.[27]

Several of the general features of the theoretical curves in Fig. 6 are observed experimentally. The data of Thomas and Pokrovskii[18] and of Chou and Wong[17] are shown as circles and triangles, respectively, where the solid (open) symbols indicate E_F^e (E_F^h). The electron Fermi energy increases at low stresses, as predicted. However, the sharp decrease in both Fermi energies which should denote σ_e is not observed. Both theoretically and experimentally $E_F^h > E_F^e$ below σ_e and above σ_h, while the reverse is true between σ_e and σ_h. The decrease in the experimental Fermi energies relative to theory at higher stresses parallels the densities in Fig. 5.

The Fermi energies can be used to predict the electric charge on electron-hole drops. An EHD can become charged if the electron and hole chemical potentials differ. Because the electron and hole contributions to the exchange-correlation energy are nearly equal,[55] the sign of the chemical potential difference is given by the difference in Fermi energies. If $E_F^h > E_F^e$ then holes are less tightly bound to the EHD than electrons; holes evaporate, leaving the drop negatively charged. From Fig. 6 we find that EHD should be negatively charged in the stress ranges below σ_e and above σ_h, approximately, and positively charged in the intermediate range. These predictions are in agreement with the detailed calculations of Kalia and Vashishta[39] for three ideal cases. Pokrovskii and Svistunova[56] found experimentally that EHD are negatively charged in unstressed Ge, become positively charged around $-\sigma \approx 2$ kgf/mm^2, and remain positively charged at least up to $-\sigma \approx 9$ kgf/mm^2. The last result is difficult to interpret since the luminescence spectra obtained by the same authors[57] indicate that E_F^h has become larger than E_F^e. Further experiments at higher stresses would help resolve this discrepancy. The experimental results for lower stresses, however, are in excellent agreement with the predictions.

We turn now to a comparison with experimental results for ⟨100⟩-stressed Si. Figure 7 shows curves for models 1 and 2 of the full width at half maximum linewidth ΔE of luminescence spectra computed for the $T=2$ K equilibrium densities. The procedure for calculating luminescence spectra at finite stress has been discussed previously.[28] We show calculations of ΔE to facilitate comparison with raw data independent of fitting procedures.

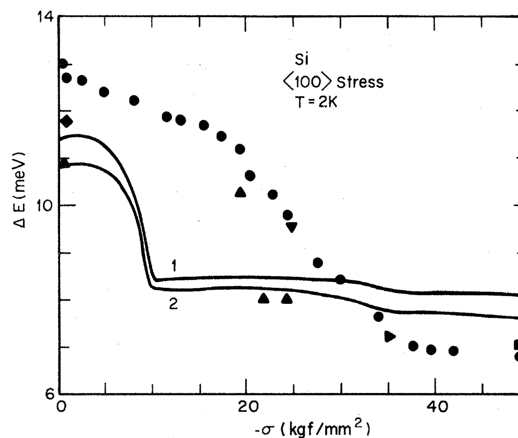

FIG. 7. Luminescence linewidth vs stress for the EHL in ⟨100⟩-stressed Si at $T=2$ K. The curves are the results for models 1 and 2. The data points are taken from Refs. 58 (◆), 59 (■), 60 (▲), 61 (▼), 62 (▶), and 20 (●).

The theoretical curves show a rapid decrease in the luminescence linewidth associated with the emptying of the upper electron valleys and a much smaller decrease associated with the emptying of the $|M_J| = \frac{3}{2}$ hole band. The figure also shows several sets of experimental points.[20,58–62] With the exception of the points from Wagner and Sauer[60] the data are in excellent agreement with each other. This is notable because the spectra have been analyzed using different procedures, in some cases[59,60,62] incorrect ones, resulting in different deduced densities for the same value of stress.[28]

Although the experimental linewidth decreases with stress, the details of the decrease differ markedly from theory. In particular, the sharp decrease associated with the critical stress σ_e is not observed experimentally. We note that there should be no ambiguity associated with the conduction-band deformation potential, since several measurements are in good agreement.[63] However, the discrepancy between experiment and theory occurs in a stress range where the equilibrium limit used in the calculation may not correspond to experimental conditions: Intervalley scattering is inhibited because $E^e_{\rm spl}$ is too small to allow the participation of TA phonons.[60] If the experiment samples non-equilibrium-limit conditions then the average observed density and linewidth will be larger than for the equilibrium limit.[25] More efficient intervalley thermalization takes place above ~ 25 kgf/mm^2 (Ref. 60). This provides a qualitative understanding for the difference between theory and experiment in the intermediate stress range.

The luminescence spectra obtained by Gourley and Wolfe were analyzed using energy- and stress-dependent hole masses.[20] Their deduced equilibrium densities are shown in Fig. 8 along with our $T = 2$ K calculations. The density variations follow the linewidths of Fig. 7. However, the break in the experimental densities at σ_e is due to the electron density of states used in the line-shape fit, since there is no corresponding feature in the linewidths. At high stresses the experimental values are significantly smaller than theory. A similar but less pronounced difference was also found for Ge in Fig. 5. We note that the results of Kirczenow and Singwi[25] for the model employing a self-consistent particle-hole (SPH) approximation[4] show better agreement with experiment at high stress. However, this agreement may be fortuitous: The SPH calculation, which was done for

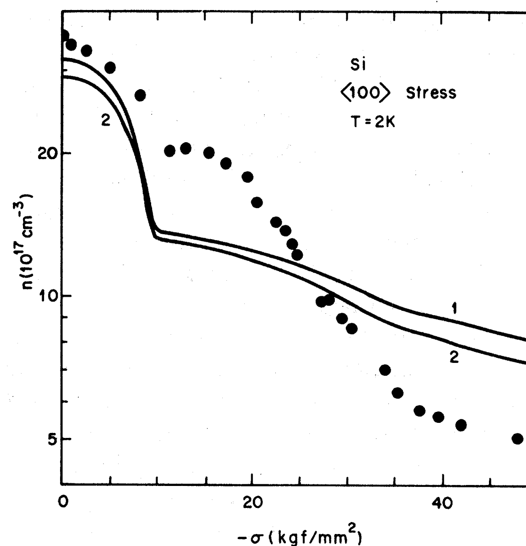

FIG. 8. Equilibrium density vs stress for Si at $T = 2$ K. The curves are the results for models 1 and 2, and the data points are from Ref. 20.

zero stress, is expected[4,5] to be inferior to an FSC calculation because it (SPH) treats only part of the problem self-consistently. The importance of the discrepancy between theory and experiment should not be underestimated, since infinite-stress theories should be better than zero-stress theories due to the simplifications in the band structure.

To assess differences in band structures, we investigated the effect of a uniform change in both electron and hole masses on the EHL equilibrium density.[27] We suppose that the masses change in the kinetic energy and that the exchange-correlation energies are unchanged. For a mass decrease of 10%, we find that the equilibrium densities decrease rather uniformly for all stresses by nearly 25% in model 1 and by $\sim 35\%$ in model 2. The Fermi energies and the luminescence linewidth have a smaller decrease, $\sim 8\%$. On the other hand, in extracting the density by fitting a luminescence spectrum, a given spectrum would be assigned a density about 15% larger. The net effect of these changes in Fig. 8 would be to bring both theoretical curves and the data nearly into coincidence at high stresses. Thus a reduction of the electron and hole masses by $\sim 10\%$ at high compressive stress could remove some of the current discrepancies between theory and experiment.

Let us examine several possibilities for changes in one or both masses. First, our calculation of the hole masses[28] ignored the effects of the split-off

valence band and fourth-order (k^4) terms which have been discussed by Hasegawa.[64] We find that including the split-off valence band results in only a small change in the density-of-states hole mass at the stresses attained in experiments: $\sim 1.7\%$ for $-\sigma = 165$ kgf/mm^2 along $\langle 100 \rangle$ in Si and for $-\sigma = 20$ kgf/mm^2 along $\langle 111 \rangle$ in Ge. In addition, this mechanism increases rather than decreases the hole mass.[65] The fourth-order terms become less important at high stresses. Second, the reduction in the average band gaps with stress should be accompanied by a decrease in the carrier masses. These decreases may be simply estimated using the $\vec{k}\cdot\vec{p}$ result $m^{-1} \sim E_g^{-1}$ and a typical value 10 meV/kbar = 1 meV mm^2/kgf for the change in E_g with stress. The relevant gaps are *direct* gaps, i.e., $E_0 \sim 0.9$ eV and $E_1 \sim 2.3$ eV in Ge (Ref. 66) and $E_0 \sim 4.2$ eV and $E_2 \sim 4.5$ eV in Si (Ref. 67). At the highest stresses attained in experiments, the masses would decrease by $\sim 1-2\%$ in Ge and $\sim 4\%$ in Si. A third possibility is the renormalization of the carrier masses within the EHL by many-body effects. It has been found both theoretically[68,69] and experimentally[70,71] that for unstressed Ge the masses within the EHL increase by $\sim 10\%$ relative to the bulk masses. However, the stress dependence of this mass renormalization is not known. We conclude that decreases in the carrier masses by as much as 10% at high stresses cannot be reliably predicted by these considerations.

The electron and hole Fermi energies for Si are shown in Fig. 9, where the solid circles indicate E_F^e and the open circles E_F^h. We find the following theoretical values for the critical stresses:

$$\left.\begin{array}{l} -\sigma_e \approx 10 \text{ kgf/mm}^2 \\ -\sigma_h \approx 37 \text{ kgf/mm}^2 \end{array}\right\} \text{Si}, \; T = 2 \text{ K}, \; \langle 100 \rangle \text{ stress} . \quad (8)$$

The qualitative theoretical behavior of E_F^e and E_F^h can be understood for Si in the same way as for Ge. We note that the dashed line which indicates E_{spl}^e crosses the experimental points near their maximum, as in Fig. 6 for Ge. This deviation from theory may be associated with non-equilibrium-limit experimental conditions in this stress range. In spite of the *quantitative* differences between theory and experiment, we note that $E_F^h > E_F^e$ at all stresses. Thus EHD should be negatively charged at all stresses in Si, in contrast to the situation for Ge. There are no experimental results concerning the charge on EHD in Si.

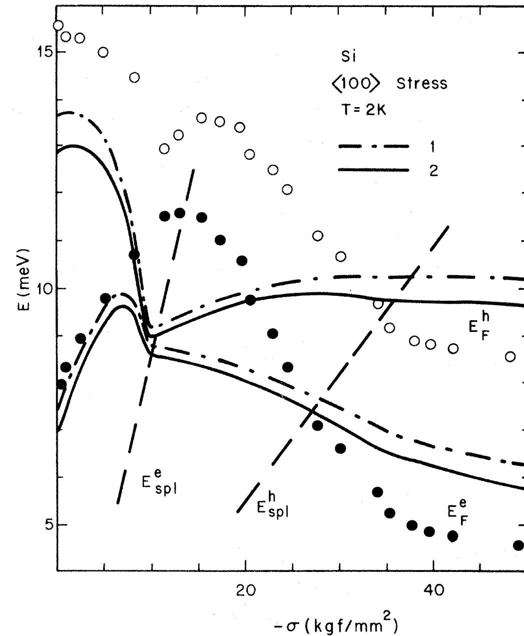

FIG. 9. Electron and hole Fermi energies vs stress for Si at $T = 2$ K. Notation for the curves is similar to Fig. 6, while the data points for E_F^e (●) and E_F^h (○) are from Ref. 20.

Two experimental measurements of the EHL binding energy are available for stressed Si. Kulakovskii *et al.*[72] found $\phi = 2 \pm 0.2$ meV at a stress $-\sigma = 48$ kgf/mm^2. We find theoretical upper limits of 2.40 meV for model 1 and 2.50 meV for model 2. In addition, Wolfe and Gourley[73] measured $\phi = 1.5 \pm 0.5$ meV at a stress $-\sigma = 90$ kgf/mm^2, compared to 1.84 meV for model 1 and 2.01 meV for model 2. The agreement between theory and experiment is satisfactory: as expected, ϕ decreases at higher stresses.

We consider finally the infinite-stress limit of the EHL in Ge and Si. Since infinite stress is impossible to attain experimentally, it is necessary to understand what constitutes a stress "high enough" that the valence-band nonparabolicity is negligible or to have a method for extrapolating to infinite stress. Our calculations show that the properties of the EHL are still changing at stresses much greater than σ_h. The $T = 2$ K equilibrium densities for Ge and Si are replotted as a function of $1/\sigma$ in Figs. 10 and 11, respectively, where the arrows indicate σ_h. Data points from the sources for Figs. 5 (Refs. 14, 16–19) and 8 (Ref. 20) are also shown. In Ge, at $-\sigma = 20$ kgf/mm^2, the largest experimental stress to date, the theoretical densities are still twice their infinite-stress values. To obtain

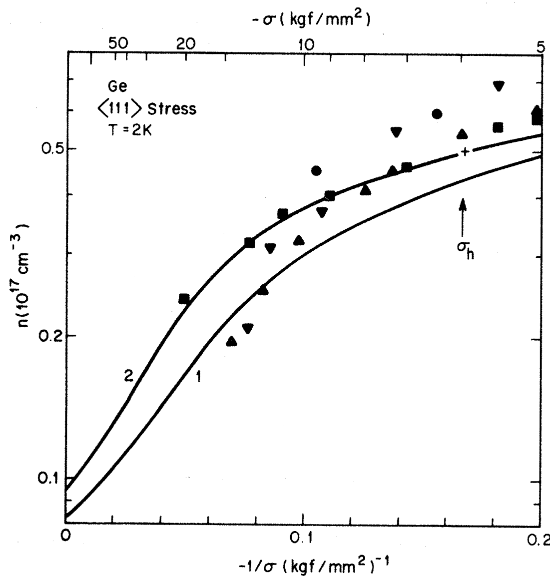

FIG. 10. Equilibrium density vs $1/\sigma$ for Ge at $T=2$ K. The curves are the results for models 1 and 2, and the data points are the same as in Fig. 5. The arrow indicates the critical stress σ_h.

densities within 20% of the infinite-stress value, stresses in the range $-\sigma \gtrsim 70$ kgf/mm^2 would be required for Ge and $-\sigma \gtrsim 150$ kgf/mm^2 for Si.

Data for somewhat lower stresses can be used, however, to extrapolate to infinite stress. For example, Fig. 10 shows that a linear extrapolation (on an n vs $1/\sigma$ semilog plot) would be appropriate for stresses greater than ~ 15 kgf/mm^2. A different extrapolation procedure used by Thomas and Pokrovskii[18] was inappropriate because it was based on only a few data points, all obtained at rather low stresses. While the data of Zarate and Timusk[19] agree well with model 2, their densities are larger than those obtained by Chou *et al.*[16,17] and should be treated with caution. Therefore, it is not possible to make a reliable extrapolation to infinite stress based on current data for Ge. For Si, it is evident from Fig. 11 that such a linear extrapolation procedure should be reasonable for stresses above ~ 40 kgf/mm^2. The data of Gourley and Wolfe[20] extend well into this range. Our extrapolation yields an infinite-stress density $n \approx 2.8 \times 10^{17}$ cm^{-3} ($T \approx 1.4$ K in the experiments).

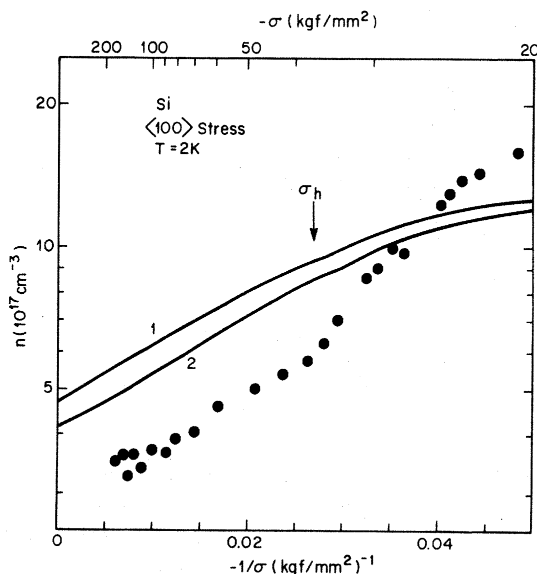

FIG. 11. As Fig. 10, for Si. The data points are from Ref. 20.

IV. RESULTS: FINITE TEMPERATURE

In this section we are interested in the variation of EHL properties with temperature. First we consider the systematic variations at low temperatures, which involve derivatives of ground-state properties. Then we consider the critical point of the electron-hole liquid-gas system. Finally, we comment briefly on scaling relations for EHL parameters.

A. Low-temperature variations; compressibility

The usual procedure for studying the properties of the EHL at low temperatures is a perturbation treatment. At sufficiently low temperatures, EHL properties vary as T^2, like any other degenerate Fermi system. The systematic low-temperature variations depend on derivatives of ground-state properties. In this section we consider four quantities: the isothermal compressibility K_T and quantities which describe the low-temperature variations of the equilibrium density (δ_n), chemical potential (δ_μ), and total Fermi energy (δ_E).

The following definition of the isothermal compressibility is valid for any density and temperature:

$$K_T^{-1} \equiv -V \left[\frac{\partial P}{\partial V} \right]_{N,T}$$

$$= 2n^2 f'(n,T) + n^3 f''(n,T) , \qquad (9)$$

where the prime denotes differentiation with respect to density at constant temperature and

$P=n^2\partial f/\partial n$. For the ground state

$$K_T(n_0)=(n_0^3 f_G'')^{-1} , \tag{10}$$

where $f_G''=f''(n_0,0)$ is the curvature of the free energy. The ground-state compressibilities for models 1 and 2 are shown as a function of stress for Ge and Si in Figs. 12 and 13, respectively. The overall increase in $K_T(n_0)$ with stress is primarily due to the decrease in n_0. At densities just above those where the upper conduction and valence bands empty, the free energy is relatively flat, resulting in peaks in the compressibility. The peaks occur just below the critical stresses σ_e and σ_h, and their size depends on how drastic the carrier redistribution is. Because the predicted increase in $K_T(n_0)$ just below σ_e is so large for both Ge and Si, experimental measurements in this range of stresses would be particularly interesting. Two measurements of the compressibility have been obtained in stressed Ge. We have found,[74] for $T=1.9$ K and $-\sigma\approx 5.5$ kgf/mm^2, that $K_T\approx 0.067\pm 0.017$ cm^2/dyn ($n\approx 0.47\times 10^{17}$ cm^{-3}), compared to a theoretical value of 0.041 cm^2/dyn for model 1. In addition, Ohyama *et al.*[75] obtained $K_T\approx 0.023\pm 0.002$ cm^2/dyn for $T=0$ and a similar but unspecified stress. Because the latter authors did not take into account the compression of the liquid by the strain well, however, we believe that their result could underestimate the true value by as much as a factor of 3.[74] In view of the complexity of the measurements, the agreement is fairly good.

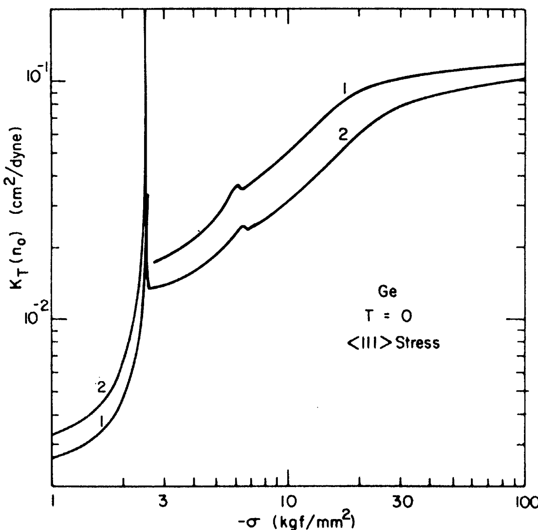

FIG. 12. Isothermal compressibility of the EHL ground state as a function of ⟨111⟩ stress in Ge, for models 1 and 2.

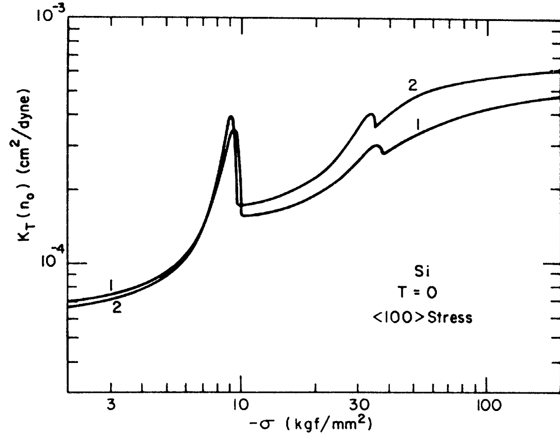

FIG. 13. As Fig. 12, for ⟨100⟩ stress in Si.

The parameters δ_n, δ_μ, and δ_E are defined from the following relations[1]:

$$n(T)=n_0[1-\delta_n(kT)^2],\ \ \delta_n \text{ in meV}^{-2} \tag{11a}$$

$$\mu(T)=\mu(0)-\delta_\mu(kT)^2,\ \ \delta_\mu \text{ in meV}^{-1} \tag{11b}$$

$$E_F(T)=E_F(0)[1-\delta_E(kT)^2],\ \ \delta_E \text{ in meV}^{-2} . \tag{11c}$$

Because of the complications due to the band splitting and nonparabolicity, we outline the derivation of these quantities. At low temperatures the kinetic energy can be written

$$f_{\text{kin}}(n,T)=f_{\text{kin}}(n,0) -\tfrac{1}{2}[\gamma_e(n)+\gamma_h(n)]T^2 , \tag{12a}$$

where

$$\gamma(n)=\frac{\pi^2}{3}k^2\frac{D(E_F(0))}{N} \tag{12b}$$

applies for electrons or holes. The low-temperature expansion is valid if

$$0<kT/E_F(T)\ll 1$$

and

$$0<kT/[E_F(T)-E_{\text{spl}}]\ll 1 .$$

For the special case $E_F=E_{\text{spl}}$, then, Eq. (12a) is invalid. For other cases, these conditions may be fulfilled by restricting the expansion to sufficiently low temperatures. The quantity γ, which is related to the heat capacity, is a monotonically decreasing function of density except in a narrow range where the occupation of the upper ν_2 bands is small (but nonzero). Thus anomalies occur just below σ_e and σ_h in quantities which depend on γ.

If the equilibrium density at the temperature T is written $n(T)=n_0+\Delta n$, then it is easy to show that

$$f'(n_0+\Delta n,T)=0$$
$$=\Delta n f''(n_0,0)$$
$$-\tfrac{1}{2}[\gamma_e'(n_0)+\gamma_h'(n_0)]T^2 , \quad (13)$$

to first order in Δn. Thus δ_n may be written

$$\delta_n=-\frac{n_0^2K_T(n_0)}{2k^2}[\gamma_e'(n_0)+\gamma_h'(n_0)] . \quad (14)$$

The results for δ_n are shown in Figs. 14(a) and 15(a). The discontinuities at σ_e and σ_h are due to a discontinuity in γ' for $E_F(0)=E_{\rm spl}$. For most stresses γ_e' and γ_h' are negative. Thus, as is familiar from unstressed Ge and Si, the EHL expands with temperature. Just below σ_e and σ_h, however, δ_n becomes negative, implying initial thermal contraction. Although the range of conditions for the thermal contraction is restricted, its observation would be very interesting.

The quantity δ_μ describes the variation in the chemical potential with temperature. At a low-temperature equilibrium density the chemical potential can be written $\mu(T)=f(n_0+\Delta n,T)$, since f is a minimum, and expanded to first order in Δn. Thus

$$\delta_\mu=\frac{1}{2k^2}[\gamma_e(n_0)+\gamma_h(n_0)] . \quad (15)$$

Results for Ge and Si are shown in Figs. 14(b) and 15(b), respectively. The enhancement just below σ_e and σ_h shows the behavior of $\gamma_e(n)$ and $\gamma_h(n)$, respectively, at the associated densities. The broader σ_e-related structures in Si, as compared to Ge, reflect the more gradual emptying of the upper electron valleys.

The quantity δ_E describes the variation in the total Fermi energy $E_F^{\rm tot}=E_F^e+E_F^h$ with temperature. There are actually two distinct contributions for each Fermi energy[1]:

$$E_F(T)=E_F(0)+\Delta E_1+\Delta E_2 . \quad (16)$$

The first is due to the change in equilibrium densi-

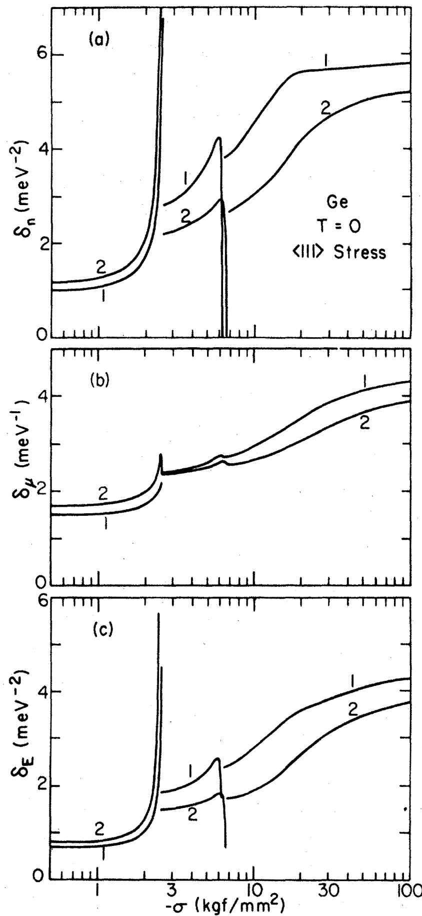

FIG. 14. (a) δ_n, (b) δ_μ, (c) δ_E as a function of $\langle 111\rangle$ stress for Ge. Models 1 and 2 are shown.

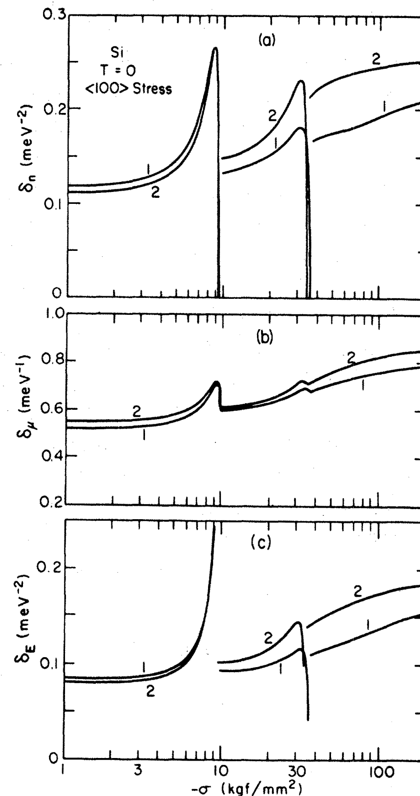

FIG. 15. As Fig. 14, for $\langle 100\rangle$ stress in Si.

ty with temperature, while the second is an explicit temperature dependence at constant density. Thus

$$\delta_E=\delta_{E1}+\delta_{E2}\ , \tag{17a}$$

where we find[27]

$$\delta_{E1}=\delta_n n_0 \frac{E_F^{e'}(0)+E_F^{h'}(0)}{E_F^e(0)+E_F^h(0)} \tag{17b}$$

and

$$\delta_{E2}=\frac{\pi^2}{6}\frac{\frac{D'(E_F^e(0))}{D(E_F^e(0))}+\frac{D'(E_F^h(0))}{D(E_F^h(0))}}{E_F^e(0)+E_F^h(0)}\ . \tag{17c}$$

In Eq. (17b) the primes denote derivatives with respect to n, while in Eq. (17c) the derivatives are with respect to E. For most stresses δ_E is dominated by δ_{E1}. Just below σ_e and σ_h, however, δ_{E2} becomes more important, because of the rapid change in the density of states at the Fermi level. The results shown in Figs. 14(c) and 15(c) are similar to the curves for δ_n. It is easy to verify that the expressions for δ_n, δ_μ, and δ_E simplify for unstressed Ge and Si to the usual expressions.[1]

Numerical results for $K_T(n_0)$ and the δ quantities are listed in Tables III and IV, respectively, where both tables list the same models and stresses. In comparing models, it is useful to remember that these quantities depend on derivatives of the free energy (or a related quantity) and sometimes on high powers of the equilibrium density. Close agreement requires very detailed similarities between the models.

Measurements of the quantities discussed in this section are sparse. Zero-stress values are listed in the table and are in reasonable agreement with theory. Feldman *et al.*[15] found $\delta_n=6.7\pm2.0$ meV^{-2} at 13 kgf/mm^2 in Ge, to be compared to theoretical values of 5.1 and 3.4 meV^{-2} for models 1 and 2, respectively. Kulakovskii *et al.*[76] found $\delta_n=0.21\pm0.3$ meV^{-2} for Si at an unspecified stress, probably in the range 50–80 kgf/mm^2. The corresponding theoretical values are ~ 0.18 and ~ 0.24 meV^{-2} for models 1 and 2, respectively. No experimental values for δ_μ or δ_E have been published for either stressed Ge or stressed Si.

B. The critical point

Thermodynamically, the definition of the critical point can be written

$$\left[\frac{\partial \mu}{\partial n}\right]_T=\left[\frac{\partial^2 \mu}{\partial n^2}\right]_T=0\ . \tag{18}$$

Thus the critical point corresponds to the inflection point in the chemical potential versus density. By performing the calculation for a plasma of electrons and holes, we assume that other species such as excitons, trions, and biexcitons are not important near the critical point. This scheme was first used by Combescot[8] and has been followed in other calculations of the critical point at zero and infinite stress.

In order to obtain meaningful results for model 1, it was necessary to modify the correlation energies. The anomalies illustrated in Fig. 1 are greatly magnified in the second and third derivatives which determine the critical point. To circumvent this mathematical problem we fitted the original model 1 correlation energies to a simple Wigner form, consisting of a single term in Eq. (6), over an intermediate density range corresponding to $r_s=2$ to 3, and then extended the calculation to higher and lower densities as needed. This procedure is reasonable since the correlation energy is expected to have a Wigner-type density dependence for $r_s>2$.[38] The modified model 1 exchange-correlation energy is shown as a dashed curve in Fig. 1.

Results for the critical temperature T_c and critical density n_c in Ge are shown in Figs. 16 and 17, respectively, while the results for Si are shown in Figs. 18 and 19. The results for models 1 and 2 are quite similar, considering the sensitivity of the calculation to details such as curvature of the correlation energy. We find gradual decreases in both T_c and n_c with stress, with a more rapid change associated with the depopulation of the upper electron valleys and a leveling off at high stresses. The reduction in T_c follows from the reduction in the liquid binding energy ϕ, while the decrease in n_c approximately parallels the decrease in the ground-state density n_0 except in the immediate vicinity of σ_e.

Numerical results for the critical point at selected values of the stress are given in Table IV, where they are compared to other calculations. We show the results of a T^2 calculation for model 5 at zero stress and model 6 at infinite stress. These models are practically identical to those used by Vashishta, Das, and Singwi[7] but the results differ substantially. This is due to an error in the calculation of Ref. 7 and those results have now been revised, in agreement with the values in the table.[36,38] We show for comparison the results of Reinecke *et al.*[30] calculated using their noninteracting fluctuation model,[29] which also uses a T^2 expansion. The values for T_c obtained in this model are lower than those obtained using the plasma model, while

TABLE IV. Selected numerical results for properties of the EHL in stressed Ge and Si at finite temperature.

Material, Stress direction	$-\sigma$ ($\mathrm{kgf/mm^2}$)	Model	δ_n ($\mathrm{meV^{-2}}$)	δ_μ ($\mathrm{meV^{-1}}$)	δ_E ($\mathrm{meV^{-2}}$)	T_c (K)	n_c ($10^{17}\ \mathrm{cm^{-3}}$)
Ge, ⟨111⟩	Zero	Expt.	0.9−1.4[a,b]	22±0.9[b]	0.71±0.14[b]	6.5−7.0[f−h]	0.5−1.0[f−h]
		5	1.24	1.69	0.92	8.18[j]	0.50[j]
		Fluc.				6.73[k]	0.66[k]
		1	0.98	1.47	0.73	6.95	0.28
		2	1.15	1.67	0.85	7.96	0.31
	3	1	2.91	2.41	1.91	5.05	0.065
		2	2.25	2.37	1.52	5.92	0.087
	7	1	3.90	2.75	2.47	4.59	0.042
		2	2.67	2.57	1.76	5.39	0.062
	20	1	5.65	3.53	3.61	3.95	0.018
		2	4.19	3.07	2.66	4.53	0.028
	Infinite	1	5.94	4.53	4.52	3.61	0.010
		2	5.41	4.14	4.07	3.99	0.014
		6	6.84	4.23	5.05	3.72[j]	0.017[j]
		Fluc.				2.91[k]	0.032[k]
Si, ⟨100⟩	Zero	Expt.	0.55±0.020[c,d]	0.3−1.7[c−e]	0.05±0.025[c−e]	26−30,[e,i] 22−24[l]	10−14[e,i,l]
		5	0.104	0.508	0.078	28.6[j]	5.1[j]
		Fluc.				23.5[k]	9.6[k]
		1	0.117	0.513	0.086	27.4	3.7
		2	0.110	0.542	0.082	26.7	3.5
	12	1	0.136	0.599	0.094	23.2	1.7
		2	0.152	0.613	0.104	22.6	1.6
	40	1	0.169	0.685	0.113	20.4	0.90
		2	0.222	0.727	0.146	20.0	0.82
	100	1	0.193	0.750	0.135	19.2	0.63
		2	0.246	0.823	0.175	18.8	0.58
	Infinite	1	0.231	0.829	0.174	18.6	0.52
		2	0.258	0.898	0.196	18.3	0.48
		6	0.246	0.864	0.186	24.4[j]	0.78[j]
		Fluc.				14.2[k]	1.42[k]

[a]T. K. Lo, Solid State Commun. 15, 1231 (1974).
[b]G. A. Thomas, T. G. Phillips, T. M. Rice, and J. C. Hensel, Phys. Rev. Lett. 31, 386 (1973).
[c]R. B. Hammond, T. C. McGill, and J. W. Mayer, Phys. Rev. B 13, 3566 (1976).
[d]M. A. Vouk and E. C. Lightowlers, J. Phys. C 8, 3695 (1975).
[e]A. F. Dite, V. D. Kulakovskii, and V. B. Timofeev, Zh. Eksp. Teor. Fiz. 72, 1156 (1977) [Sov. Phys.—JETP 72, 604 (1977)].
[f]G. A. Thomas, T. M. Rice, and J. C. Hensel, Phys. Rev. Lett. 33, 219 (1974).
[g]W. Miniscalco, C.-C. Huang, and M. B. Salamon, Phys. Rev. Lett. 39, 1356 (1977).
[h]G. A. Thomas, J. B. Mock, and M. Capizzi, Phys. Rev. B 18, 4250 (1978).
[i]J. Shah, M. Combescot, and A. H. Dayem, Phys. Rev. Lett. 38, 1497 (1977).
[j]Computed using T^2 expansion. The values differ from those given in P. Vashishta, S. G. Das, and K. S. Singwi, Phys. Rev. Lett. 33, 911 (1974), as explained in the text.
[k]Computed using droplet-fluctuation model. T. L. Reinecke, M. C. Lega, and S. C. Ying, Phys. Rev. B 20, 1562 (1979).
[l]A. Forchel, B. Laurich, G. Moersch, W. Schmid, and T. L. Reinecke, Phys. Rev. Lett. 46, 678 (1981).

the values for n_c are consistently larger. Within the plasma model, the T^2 expansion overestimates both T_c and n_c, compared to the corresponding exact-T calculation. Other theoretical estimates[8,9,30,77] of the critical point in unstressed or infinitely stressed Ge and Si using different approximations for the exchange-correlation energy are in remarkably good agreement with the values in Table IV. Also, Liu and Liu[23] have calculated the critical point at two values of stress, using a T^2

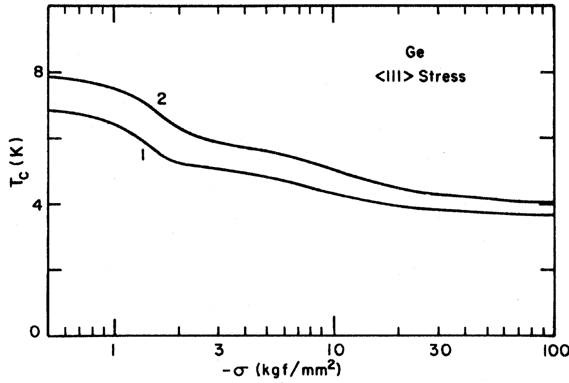

FIG. 16. EHL critical temperature vs ⟨111⟩ stress in Ge, according to models 1 and 2.

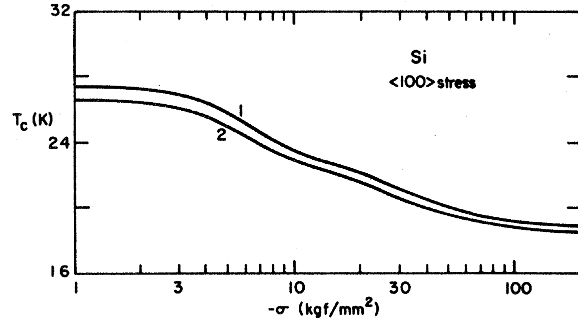

FIG. 18. EHL critical temperature vs ⟨100⟩ stress in Si, for models 1 and 2.

expansion for the kinetic energy. Taking this into account, their results are in reasonable agreement with our calculations for the same stresses.

We wish to reiterate that the low-T expansion is only valid if $0<kT/E_F \ll 1$ and $0<kT/(E_F-E_{\rm spl}) \ll 1$ for both electrons and holes. We find that these conditions are violated at the critical point for all stresses in both Ge and Si: The ratios fall outside the ranges (0−0.25) and (0−0.75) for models 1 and 2, respectively, in Ge and outside the range (0−1) for both models in Si. In view of this, we find it surprising that the differences between T^2 and exact-T calculations are not larger.

With our results for T_c and n_c we can justify *a posteriori* the use of a $T=0$ exchange-correlation energy. At the critical point this requires $kT_c/(\hbar\omega_{\rm pc}) \ll 1$, where

$$\omega_{\rm pc}=[4\pi n_c e^2(m_{\rm oe}^{-1}+m_{\rm oh}^{-1})]^{1/2} .$$

We find that this quantity is less than 0.1 for all stresses for both models in Ge and Si.

Experimental measurements of the critical point in unstressed Ge and Si are listed in Table IV. Measurements for stressed Ge include those of Furneaux *et al.*[54] ($T_c=4.7-5.7$ K for $-\sigma\approx 6$ kgf/mm^2) and Feldman *et al.*[15] ($T_c=3.5\pm0.5$ K and $n_c=7.7\pm2.0\times10^{15}$ cm^{-3} for $-\sigma=13$ kgf/mm^2). These measurements are in reasonable agreement with the present calculations. In ⟨100⟩-stressed Si, Forchel *et al.*[62] found $T_c=14.0\pm0.5$ K and $n_c=1.8\pm0.3\times10^{17}$ cm^{-3} for $-\sigma=35$ kgf/mm^2. Kulakovskii *et al.*[76] found $T_c=14\pm1.5$ K for an unspecified stress, probably in the range $-\sigma=50-80$ kgf/mm^2. Finally, Gourley and Wolfe[20,73] find $T_c=12-22$ K for $-\sigma=90$ kgf/mm^2 and $T_c\gtrsim 20$ K for $-\sigma=163$ kgf/mm^2. Until the large experimental discrepancies are

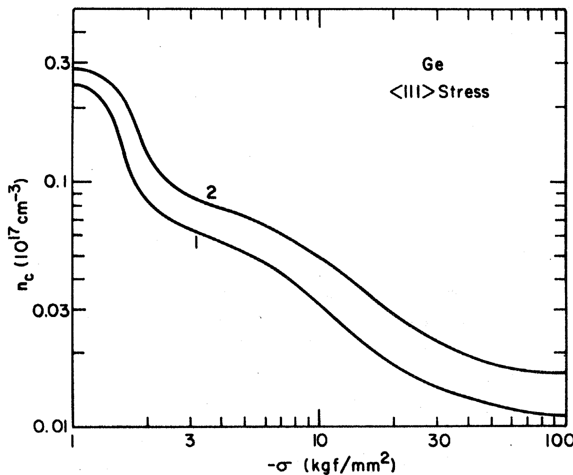

FIG. 17. EHL critical density vs ⟨111⟩ stress in Ge, for models 1 and 2.

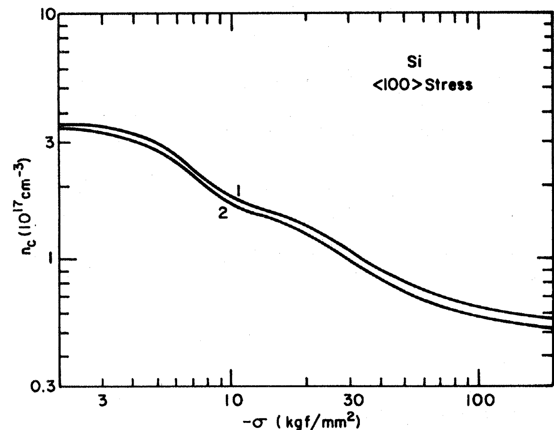

FIG. 19. EHL critical density vs ⟨100⟩ stress in Si, according to models 1 and 2.

resolved it is difficult to make meaningful comparisons with theory.

C. Scaling relations

We comment briefly on scaling relations of properties of electron-hole liquids. An early suggestion was made[1] that certain combinations of EHL properties should scale from one system (i.e., band structure) to another. More recently, Reinecke and Ying[78] have proposed on the basis of theoretical arguments a revised set of scaling quantities. They assume that the conduction and valence bands are parabolic and that the exchange-correlation energy can be written $f_{\text{excor}} \sim n^p$, using the same value of p for different systems. In this model the proposed scaling quantities are n_c/n_0, $|f_G|/kT_c$, and $\kappa T_c/n_0^p(\kappa/\mu)^{1-3p}$, where μ is an optical average of the electron and hole masses. In addition, they propose that $p \approx 0.25$.

The validity of these ideas can easily be tested by computing the above quantities as a function of stress for Ge and Si, using models 1 and 2. We find the following ranges of values:

$$\frac{n_c}{n_0} \approx 0.08-0.14\,, \tag{19a}$$

$$\frac{|f_G|}{kT_c} \approx 7.8-10.2\,, \tag{19b}$$

$$\frac{T_c\kappa}{n_0^{1/4}}\left[\frac{\kappa}{\mu}\right]^{1/4} \approx 0.016-0.025\ \text{K cm}^{3/4}\,. \tag{19c}$$

We have excluded from consideration a small range of stresses around σ_e, where we find somewhat larger variations. The ratio n_c/n_0, in particular, changes rapidly in the vincinity of σ_e, as can be seen by comparing Figs. 5 and 8 with Figs. 17 and 19. The values obtained for these quantities using the fluctuation model[78] are different from the present values obtained using the plasma model for the critical point. The experimental values given in Tables III and IV for unstressed Ge, for which there is good agreement among different experiments, seem to favor the fluctuation model. However, the variations with stress, exchange-correlation energy model, and material from Eq. (19) are expected to persist. We find, for example, that the extreme values for the scaling quantities are not necessarily obtained at zero or infinite stress. We conclude that the "universal" scaling quantities, originally proposed for model systems, have somewhat more variation when considered in detail as functions of stress. This undoubtedly occurs because the simple form for the free energy used in Ref. 78 is not applicable at finite stresses.

ACKNOWLEDGMENTS

I am grateful for assistance and advice from R. S. Markiewicz during the early phases of this work, and for many discussions with P. Vashishta concerning his unpublished calculations. I would also like to thank P. L. Gourley and H. G. Zarate for sending their experimental results prior to publication. D. E. Aspnes, J. C. Hensel, and T. M. Rice provided helpful comments on the manuscript. The work performed at Berkeley was supported in part by the Director, Office of Energy Research, Office of Basic Energy Sciences, Material Sciences Division of the U. S. Department of Energy under Contract No. W-7405-ENG-48.

---

*Present address: Xerox Palo Alto Research Center, Palo Alto, California 94304.

[1]For reviews, see the articles by T. M. Rice, in *Solid State Physics,* edited by H. Ehrenreich, F. Seitz, and D. Turnbull (Academic, New York, 1977), Vol. 32, p. 1, and J. C. Hensel, T. G. Phillips, and G. A. Thomas, *ibid.,* p. 88.
[2]M. Combescot and P. Nozières, J. Phys. C 5, 2369 (1972).
[3]W. F. Brinkman and T. M. Rice, Phys. Rev. B 7, 1508 (1973).
[4]P. Bhattacharyya, V. Massida, K. S. Singwi, and P. Vashishta, Phys. Rev. B 10, 5127 (1974).
[5]P. Vashishta, P. Bhattacharyya, and K. S. Singwi, Phys. Rev. B 10, 5108 (1974).
[6]P. Vashishta, R. K. Kalia, and K. S. Singwi, *Physics of Highly Excited States in Solids,* Vol. 57 of *Lecture Notes in Physics,* edited by M. Ueta and Y. Nishina (Springer, Heidelberg, 1976), p. 187.
[7]P. Vashishta, S. G. Das, and K. S. Singwi, Phys. Rev. Lett. 33, 911 (1974).
[8]M. Combescot, Phys. Rev. Lett. 32, 15 (1974).
[9]G. A. Thomas, T. M. Rice, and J. C. Hensel, Phys. Rev. Lett. 33, 219 (1974).
[10]V. S. Bagaev, T. I. Galkina, O. V. Gogolin, and L. V. Keldysh, Zh. Eksp. Teor. Fiz. Pis'ma Red. 10, 309 (1969) [JETP Lett. 10, 195 (1969)]; V. S. Bagaev, T. I. Galkina, and O. V. Gogolin, *Proceedings of the*

Tenth International Conference on the Physics of Semiconductors, Cambridge, 1970, edited by S. P. Keller, J. C. Hensel, and F. Stern (U.S. AEC Dir. Tech. Information, Oak Ridge, Tenn., 1970), p. 500.

[11]C. Benôit à la Guillaume, M. Voos, and F. Salvan, Phys. Rev. B 5, 3079 (1972).

[12]B. M. Ashkinadze, I. P. Kretsu, A. A. Patrin, and I. D. Yaroshetskii, Fiz. Tekh. Poluprovodn. 4, 2206 (1970) [Sov. Phys.—Semicond. 4, 1897 (1970)].

[13]R. S. Markiewicz, J. P. Wolfe, and C. D. Jeffries, Phys. Rev. Lett. 32, 1357 (1974); 34, 59(E) (1975); J. P. Wolfe, R. S. Markiewicz, C. Kittel, and C. D. Jeffries, Phys. Rev. Lett. 34, 275 (1975); C. D. Jeffries, J. P. Wolfe, S. M. Kelso, R. S. Markiewicz, and J. E. Furneaux, J. Lumin. 12, 659 (1976).

[14]J. P. Wolfe, R. S. Markiewicz, S. M. Kelso, J. E. Furneaux, and C. D. Jeffries, Phys. Rev. B 18, 1479 (1978).

[15]B. J. Feldman, H.-h. Chou, and G. K. Wong, Solid State Commun. 24, 521 (1977).

[16]B. J. Feldman, H.-h. Chou, and G. K. Wong, Solid State Commun. 26, 209 (1978).

[17]H.-h. Chou and G. K. Wong, Phys. Rev. Lett. 41, 1677 (1978).

[18]G. A. Thomas and Ya. E. Pokrovskii, Phys. Rev. B 18, 864 (1978).

[19]H. G. Zarate, Ph.D. thesis, McMaster University, 1981 (unpublished); H. G. Zarate and T. Timusk, Bull. Am. Phys. Soc. 26, 487 (1981) and unpublished.

[20]P. L. Gourley, Ph.D thesis, University of Illinois at Urbana-Champaign, 1980 (unpublished); P. L. Gourley and J. P. Wolfe, Phys. Rev. B 24, 5970 (1981).

[21]R. S. Markiewicz and S. M. Kelso, Solid State Commun. 25, 275 (1978).

[22]L. Liu, Solid State Commun. 25, 805 (1978).

[23]L. Liu and L. S. Liu, Solid State Commun. 27, 801 (1978).

[24]G. Kirczenow and K. S. Singwi, Phys. Rev. B 19, 2117 (1979).

[25]G. Kirczenow and K. S. Singwi, Phys. Rev. B 21, 3597 (1980).

[26]Some of the results are indicated in S. M. Kelso, Bull. Am. Phys. Soc. 24, 343 (1979).

[27]S. M. Kelso, Ph.D. thesis, University of California, Berkeley, 1979 (unpublished).

[28]S. M. Kelso, Phys. Rev. B 25, 1116 (1982).

[29]T. L. Reinecke and S. C. Ying, Phys. Rev. B 13, 1850 (1976).

[30]T. L. Reinecke, M. C. Lega, and S. C. Ying, Phys. Rev. B 20, 1562 (1979); 20, 5404 (1979).

[31]G. Kirczenow and K. S. Singwi, Phys. Rev. Lett. 42, 1004 (1979); Phys. Rev. B 20, 4171 (1979).

[32]K. S. Singwi and M. P. Tosi, Phys. Rev. B 23, 1640 (1981).

[33]T. M. Rice, in *Proceedings of the Twelfth International Conference on the Physics of Semiconductors, Stuttgart, 1974,* edited by M. H. Pilkuhn (Teubner, Stuttgart, 1974), p. 23; Contemp. Phys. 20, 241 (1979); Ref. 1.

[34]J. H. Rose, H. B. Shore, and T. M. Rice, Phys. Rev. B 17, 752 (1978).

[35]G. Kirczenow and K. S. Singwi, Phys. Rev. Lett. 41, 326 (1978); 41, 1140(E) (1978).

[36]P. Vashishta, R. K. Kalia, and K. S. Singwi, in Electron-Hole Droplets in Semiconductors, edited by L. V. Keldysh and C. D. Jeffries (North-Holland, Amsterdam, in press); P. Vashishta and R. K. Kalia Phys. Rev. B 25, 6492 (1982).

[37]M. Combescot, Phys. Rev. B 10, 5045 (1974).

[38]P. Vashishta (private communication).

[39]R. K. Kalia and P. Vashishta, Phys. Rev. B 17, 2655 (1978).

[40]The form of the correlation energy is very similar to that given in Ref. 39 except that the power series contains more terms and is valid for a wider range of densities.

[41]H. Büttner, *Festkörperprobleme XIII,* edited by H. J. Queisser (Pergamon, Vieweg, 1973), p. 145; E. P. Wigner, Trans. Faraday Soc. 34, 678 (1938).

[42]A controversy concerning the best values of the deformation potentials for Si apparently remains unresolved [J. C. Hensel (private communication)].

[43]W. Kohn and J. M. Luttinger, Phys. Rev. 97, 1721 (1955); 98, 915 (1955).

[44]N. O. Lipari and M. Altarelli, Phys. Rev. B 15, 4883 (1977).

[45]V. I. Sidorov and Ya. E. Pokrovskii, Fiz. Tekh. Poluprovodn. 6, 2405 (1972) [Sov. Phys.—Semicond. 6, 2015 (1973)].

[46]K. L. Shaklee and R. E. Nahory, Phys. Rev. Lett. 24, 942 (1970).

[47]T. Ohyama, T. Sanada, and E. Otsuka, Phys. Rev. Lett. 33, 647 (1974).

[48]B. M. Ashkinadze, I. P. Kretsu, A. A. Patrin, and I. D. Yaroshetskii, Phys. Status Solidi B 46, 495 (1971).

[49]E. A. Andryushin, O. A. Gel'fond, and A. P. Silin, Fiz. Tverd. Tela 22, 1418 (1980) [Sov. Phys.—Solid State 22, 827 (1980)].

[50]A. A. Kastal'skii, Fiz. Tverd. Tela 20, 1241 (1978) [Sov. Phys.—Solid State 20, 715 (1978)].

[51]F. Bassani and D. Brust, Phys. Rev. 131, 1524 (1963).

[52]P. Merle, D. Auvergne, H. Mathieu, and J. Chevallier, Phys. Rev. B 15, 2032 (1977).

[53]K. Y. Cheng, G. L. Pearson, R. S. Bauer, and D. J. Chadi, Bull. Am. Phys. Soc. 21, 365 (1976).

[54]J. E. Furneaux, R. S. Markiewicz, and S. M. Kelso, Bull. Am. Phys. Soc. 22, 270 (1977).

[55]T. M. Rice, Phys. Rev. B 9, 1540 (1974).

[56]Ya. E. Pokrovskii and K. I. Svistunova, Zh. Eksp. Teor. Fiz. Pis'ma Red. 19, 92 (1974) [JETP Lett. 19, 56 (1974)]; Fiz. Tverd. Tela (Leningrad) 16, 3399 (1974) [Sov. Phys.—Solid State 16, 2202 (1975)]; *Proceedings of the Twelfth International Conference on the Physics of Semiconductors, Stuttgart, 1974,* edited by M. H. Pilkuhn (Teubner, Stuttgart, 1974), p. 71.

[57]The luminescence spectra obtained by Ya. E. Pokrovskii and K. I. Svistunova, Zh. Eksp. Teor. Fiz. 68, 2323 (1975) [Sov. Phys.—JETP 41, 1161 (1976)] are analyzed in Ref. 18.

[58]R. B. Hammond, T. C. McGill, and J. W. Mayer, Phys. Rev. B 13, 3566 (1976).

[59]V. D. Kulakovskii, V. B. Timofeev, and V. M. Edel'shtein, Zh. Eksp. Teor. Fiz. 74, 372 (1978) [Sov. Phys.—JETP 47, 193 (1978)]; V. M. Edel'shtein, V. D. Kulakovskii, and V. B. Timofeev, *Physics of Semiconductors, 1978,* edited by B. L. H. Wilson (Institute of Physics, London, 1979), Vol. 43, p. 383.

[60]J. Wagner and R. Sauer, Phys. Status Solidi B 94, 69 (1979).

[61]J. Wagner, A. Forchel, and R. Sauer, Solid State Commun. 36, 917 (1980).

[62]A. Forchel, B. Laurich, G. Moersch, W. Schmid, and T. L. Reinecke, Phys. Rev. Lett. 46, 678 (1981).

[63]The measurements of Ξ_u in the following papers differ by only $\sim 10\%$: I. Balslev, Phys. Rev. 143, 636 (1966); L. Laude, F. H. Pollak, and M. Cardona, Phys. Rev. B 3, 2623 (1971); I. P. Akimchenko and V. A. Vdovenkov, Fiz. Tverd. Tela 11, 658 (1969) [Sov. Phys.—Solid State 11, 528 (1969)]; K. Murase, K. Enjouji, and E. Otsuka, J. Phys. Soc. Jpn. 29, 1248 (1970).

[64]H. Hasegawa, Phys. Rev. 129, 1029 (1963).

[65]J. C. Hensel and G. Feher, Phys. Rev. 129, 1041 (1963); J. C. Hensel and K. Suzuki, Phys. Rev. B 9, 4219 (1974).

[66]D. E. Aspnes, Phys. Rev. B 12, 2297 (1975).

[67]A. Daunois and D. E. Aspnes, Phys. Rev. B 18, 1824 (1978).

[68]T. M. Rice, Nuovo Cimento B 23, 226 (1974).

[69]M. Rösler and R. Zimmermann, Phys. Status Solidi B 67, 525 (1975).

[70]H. L. Störmer, R. W. Martin, and J. C. Hensel, *Proceedings of the Thirteenth International Conference on the Physics of Semiconductors, Rome, 1976,* edited by F. G. Fumi (Tipografia Marves, Rome, 1976), p. 950; R. W. Martin, H. L. Störmer, W. Ruhle, and D. Bimberg, J. Lumin. 12/13, 645 (1976); H. L. Störmer and R. W. Martin, *Proceedings of the Conference on the Application of High Magnetic Fields In Semiconductor Physics, Oxford, 1978,* edited by J. F. Ryan (Clarendon Laboratory, Oxford, 1978), p. 269.

[71]V. I. Gavrilenko, V. L. Kononenko, T. S. Mandel'shtam, and V. N. Murzin, Zh. Eksp. Teor. Fiz. Pis'ma Red. 23, 701 (1976) [JETP Lett. 23, 645 (1976)].

[72]The value for ϕ obtained in Ref. 59 should be fairly accurate in spite of the incorrect procedure used to analyze the EHL line shape, since one is concerned only with the location of the high-energy edge of the spectrum.

[73]J. P. Wolfe and P. L. Gourley, *Physics of Semiconductors, 1978,* edited by B. L. H. Wilson (Institute of Physics, London, 1979), Vol. 43, p 379.

[74]S. M. Kelso, Phys. Rev. B (in press).

[75]T. Ohyama, I. Honbori, and E. Otsuka, J. Phys. Soc. Jpn. 48, 1559 (1980).

[76]V. D. Kulakovskii, I. V. Kukushkin, and V. B. Timofeev, Zh. Eksp. Teor. Fiz. 78, 381 (1980) [Sov. Phys.—JETP 51, 191 (1980)].

[77]W. D. Kraeft and W. Fennel, Phys. Status Solidi B 73, 487 (1976).

[78]T. L. Reinecke and S. C. Ying, Phys. Rev. Lett. 43, 1054 (1979).